Garzon-Hernandez S., Garcia-Gonzalez D. & Arias A. (2018). Multi-impact mechanical behaviour of short fibre reinforced composites. *Composite Structures*, vol. 202, pp. 241-252.

DOI: 10.1016/j.compstruct.2018.01.070

Multi-impact mechanical behaviour of short fibre reinforced composites

S. Garzon-Hernandez[a]*, D. Garcia-Gonzalez[a,b], A. Arias[a]

[a]Department of Continuum Mechanics and Structural Analysis, **University Carlos III of Madrid**, Avda. de la Universidad 30, 28911 Leganés, Madrid, Spain

[b]Department of Engineering Science, **University of Oxford**, Parks Road, Oxford OX1 3PJ, UK

***Corresponding author:** sgarzon@ing.uc3m.es

Abstract: High velocity transverse impact on reinforced composites is a matter of interest in the automotive, aeronautical and biomedical sectors. Most existing studies have addressed this problem by single isolated impacts; however, this work deals with the distinction between single, sequential and simultaneous impacts on composite structures. This paper proposes an experimental methodology to study the mechanical behaviour of materials under single and multi-impact loadings. The overall objective is to investigate the mechanical response of short carbon fibre reinforced PEEK when subjected to single and multiple high velocity impacts. Experimental tests are conducted covering impact velocities from 90 m/s to 470 m/s. Energy absorption, damage extension and failure mechanisms are compared to assess additive and cumulative effects of high velocity impact scenarios. Experimental results show that the specific deformation and fracture mechanisms observed during multi-hitting events change with impact velocity. Compared to the behaviour of unreinforced thermoplastics, short fibre reinforced composites present significant limitations at velocities close to ballistic limit, but multi-hit capability is observed at high impact velocity when the damage is mainly local. As key conclusion, the ballistic limit obtained in single test cannot be extrapolated to sequential and simultaneous impact tests. Multi-impact tests, especially close to the ballistic limit, are necessary to guarantee the structural integrity of composite structures in realistic impact scenarios.

Keywords: Multi-impact; Short fibre reinforced thermoplastics; PEEK composites; Perforation; Brittle failure, High velocity impact;

1. Introduction

Thermoplastic polymers have experienced an increasing interest due to their good mechanical properties and possibilities in terms of manufacturing [1-3]. Furthermore, thermoplastics can be reinforced by incorporating long fibres, short fibres and particulate reinforcement, thus improving their mechanical properties [4,5]. Thermoplastic composites are currently employed in different industries for a wide variety of applications. Among these industries, the presence of thermoplastic composites stands out in the automotive, aeronautical and biomedical [6] sectors, where metals are being replacing due to their good properties and biocompatibility [7]. In this regard, particular attention has been paid to thermoplastic polymers reinforced with short fibres (SFR thermoplastics) because of their advantages for customized and complex-geometry products, especially useful in biomedical applications [8]. One of the major problems of SFR thermoplastics is that, although an increase in stiffness is achieved with respect to unfilled thermoplastics, the addition of short fibre reinforcement generally results in a reduction of ductility leading to the embrittlement of the composite [9,10]. This can suppose a limitation in applications that are potentially exposed to impact loading, especially common in automotive and aeronautical components, and in external human prosthesis [11].

The mechanical response of materials against impact loading has been mainly addressed by single impact testing [6,12-16]. However, in real scenarios, many structures are potentially exposed to multi-impact loading such as in automotive and aeronautical applications due to hailstorms or particle multi-hitting [17-19]. In addition, potential prosthetic devices provide structural support for the body and they must be able to absorb enough energy above its ultimate strength without showing fracture [20]. Therefore, it is essential to study the effect of reduced ductility in order to determine the levels of energy absorption of prostheses, such as cranial implants and hip systems [21], in dynamic conditions with energy levels commonly generated in a fall or accident.

The importance of studying materials under repeated or simultaneous impacts has been allude by several authors [18,19,22-24], although only few works can be found in literature. An impact

series is considered sequential when the time-hit interval is sufficiently long to avoid synergistic effects from stress waves interaction [17]. These sequential impacts can be understood as the repetition of impact over the same area until failure. On the other hand, an impact series is considered simultaneous when stress and shock wave interaction is expected. In this regard, there are only few works that study the mechanical response of materials against more than one projectile impacting sequentially or at the same time and, to the authors' knowledge, these are focussed uniquely on metal materials [18] and long fibre composites [24]. In such works, lower impact energy thresholds have been found to result in failure in comparison with the expected energies from single impact studies. This reduction in critical impact energies arises from combined effects of stress wave interactions and stress concentration due to previous damage. Therefore, the analysis of the mechanical response of materials under sequential and simultaneous impacts is essential to determine their suitability for a specific application potentially exposed to impact loading.

To the authors' knowledge, there is no available work in the literature on the mechanical response of SFR composites under multi-impact loading, scenario where synergetic effects arising from stress wave interactions are expected leading to reduced impact energy levels to reach material failure. The main aim of the research presented in this paper is to propose an experimental methodology to study the mechanical behaviour of SFR thermoplastics under single and multi-impact loadings. To this end, we present experiments on plates manufactured with short carbon fibre reinforced polyether-ether-ketone (SCFR PEEK) composites. These experiments cover three potential impact scenarios: single impact, sequential impacts, and simultaneous impacts. In sequential and simultaneous tests, the impact localisation is controlled with a distance between impacts greater than twice the diameter of the projectile employed. The impact energy ranges from 10 J to 184 J, covering an energy range equivalent to usual impact loading observed in for industrial applications. The results obtained herein show the need to take into account synergetic effects of stress wave interactions and bending due to multi-hits as well as stress concentrations due to previous damage, and highlight potential limitations of

components subjected to impact whose suitability has been only evaluated by single impact testing.

2. Materials and methods

2.1. Baseline material

PEEK stands out among thermoplastic polymers used as composites matrix due to its properties such as good thermal stability, chemical resistance, low flammability and excellent mechanical properties [25,10]. In this regard, semi-crystalline polymers show a complex mechanical behaviour that presents a strong non-linearity and depends on strain rate, temperature, stress state, large deformations and plastic flow [3]. In addition and for dynamic processes, thermal softening also influences the deformation process of thermoplastic polymers [2], as observed in other ductile materials [26]. Moreover, fibre reinforced semi-crystalline composites are used in applications that requires excellent impact performance due to the incorporation of short fibres into a thermoplastic matrix permits to improve the stiffness and strength [27]. Despite the good mechanical properties of SFR polymers, the fibres distribution along these composites often presents dispersion and disorientation, not providing the advantages of unidirectional long fibre composites [10]. However, SFR thermoplastics offer excellent advantages in their manufacturing process, which allows different possibilities such as extrusion or injection moulding [28]. Extrusion and injection moulding process lead to a preferred orientation along the mould filling direction [29]. Among the different materials used for the fibre reinforcement, carbon fibres are the most commonly employed in load-bearing components [30] In this regard, carbon fibre reinforcement is one of the most widely used for PEEK based composites due to its strong interfacial interaction with PEEK matrix [31].

In this work, we chose PEEK reinforced with PAN short carbon fibres 30 % in weight, denominated CF30 PEEK, as baseline material. Several plates were manufactured by injection moulding technology and were purchased measuring 130x130x3 mm^3. The diameter and length of the fibres were 7 μm and 200 μm respectively. This reinforcement leads to an increase of the tensile elastic modulus up to more than seven times the value of unfilled PEEK and doubles the failure strength value [16]. Previous experimental results show a preferred fibre orientation

mainly aligned in the injection flow direction, IFD, resulting in anisotropy with higher stiffness in the IFD [10,16]. In addition, an enhanced behaviour has been reported under compressive loading with respect to tensile loading. The main mechanical properties of this material are shown in Table 1. Regarding the fracture in SFR composites subjected to impact loading, this occurs as the result of a variety of complex damage mechanisms such as fibre cracking, fibre debonding and pull-out, plastic localisation and ductile fracture due to void growth and coalescence in the matrix [29].

2.2. Experimental method

In this paper, a series of single, sequential and simultaneous impacts were conducted on SCFR PEEK plates with a fibre weight fraction of 30%. These tests were performed using rigid spherical steel projectiles with a mass of $m_p = 1.71$ g and a diameter of $\emptyset_p = 7.5$ mm. The setup used for the tests is shown in Fig. 1. The active area of all plates was reduced to 100x100 mm^2 in order to impose boundary conditions that avoid sliding and ensure a correct clamping of the specimen, Fig. 2.

The measurement of the impact and residual velocities was carried out with two high-speed video cameras (Photron Ultima APX-RS) that were placed in both sides of the target plate during all the tests. In addition, two 1200 W HMI lamps were used to adequate the lighting. The cameras were configured to obtain 70,000 frames per second (fps) for simultaneous impact tests and 100,000 for single and sequential impact tests and, with the aim of better understanding the ultimate deformation state after impact, a reference grid composed by 1x1 cm^2 squares was drawn in each plate.

Single tests

Single impact tests provide information about the deformation and failure mechanisms that govern the perforation process. These consist of a unique projectile impact and allow for a first analysis of the mechanical response of the material under impact loading. These tests were

conducted on SCFR PEEK plates covering an initial impact velocity of $90 \leq V_0 \leq 470$ m/s. The projectiles were launched at the centre of the plates to minimize the influence of the boundary conditions. The setup used for these tests was a gas gun capable to shoot a rigid spherical projectile perpendicularly to the specimen tested.

Multi-impact test

The term multi-impact has been defined by some authors as the repetition of impacts over the same area until failure [17, 19], whereas by other authors as a near-simultaneous impact using a fragmentation devise with a random impact localisation [32,33]. In this work, two different tests were carried out controlling the localisation of impact in both.

Sequential tests

Sequential impact test consists of various single tests conducted at the same impact velocity and on the same specimen but in different localisation. The velocity range was the same used for single tests. These provide information about the influence of a potential previous damage on the mechanical impact response of the material. Thus, after having performed the first shot corresponding to the single test, other two projectiles were shot on the same target following the sequence: the second one on the left and the third one on the right of first impact, with a distance between localisation of impacts greater than twice the diameter of the projectile. The setup used for single tests was also employed to perform the sequential test. The given pressure to the gas gun was remained constant in order to obtain a similar impact velocity for the three shots.

Simultaneous tests

Simultaneous test consists of three projectiles impacting at the same time on the target (time between impacts of the other of 10 μs). These tests allow for the analysis of synergetic effects due to stress waves interaction that could lead to failure at lower energies than the ones needed in sequential tests. In order to compare the absorbed energy capability of the material depending on the impact loading conditions (single, sequential or simultaneous impacts), the velocities

selected for simultaneous multi-impact tests were chosen within the energy range covered in the previous test.

Moreover, these tests required the development of a new experimental methodology. In this regard, due to the absence of specific barrels for the multi-impact test, a structure similar to a bullet called sabot was employed and shot using a pneumatic gas canyon. The principal function of the sabot is to accelerate the three projectiles while their respective position in maintained [34]. Different sabot designs were manufactured by 3D printing with the aim of determining the optimal method to guarantee that, after colliding against the stripper, the sabot was not broken into pieces that could impact the target causing extended damage. To this end, the optimal solution found corresponds to a brittle sabot of PLA, whose interior was filled with elastomer. Different configurations of the projectiles distribution into the sabot were tested. After colliding against the stripper, the projectiles are spread out following a pattern with a great degree of repeatability.

3. Results

3.1. Introduction

In this section, we present the experimental results for each of the different tests carried out: single, sequential and multi-impact, in terms of residual velocity, energy absorption capability, creation of free surfaces created and fracture mode. The impact events were recorded and then post-processed using Photron FASTCAM Viewer software to provide the impact and residual velocities as well as the deflection and failure processes. Based on these measurements, the kinematic impact energy E_0 and the energy W transferred to the composite plate can be estimated trough Eq. (1) and Eq. (2), respectively, to analyse the energy capability.

$$E_0 = \frac{1}{2} m_p V_0^2 \tag{1}$$

$$W = \frac{1}{2} m_p \left(V_0^2 - V_r^2 \right) \tag{2}$$

where m_p is the mass of the projectile and V_0 and V_r are the impact and residual velocities, respectively.

The ballistic limit, defined as the maximum value of the initial impact velocity which induces a residual velocity equal to zero, is determined from singles tests. This ballistic limit cannot be extrapolated to the sequential and simultaneous tests because the interaction between cracks (in the case of sequential tests) and waves (in the case of multi-impact tests) can produce the penetration of the projectiles at impact velocities below the ballistic limit. Previous impact studies on these materials have corroborated by C-scan techniques the creation of free surfaces as a result of impact process [16]. Therefore, the damaged area is defined herein as the free surface areas bounded by the cracks and the pull-out area due to projectile penetration (when the ballistic limit is overcome or when the interaction between cracks results in a pull-out area), Fig. 3. In this regard, a quantification of damage extent, defined in this work as the area delimited by free surfaces created, was estimated. Note that, due to the damaged area is bigger in the rear part of the plate for all tests due to lower tensile fracture stress, all the results in these terms are referred to the rear part.

3.2. Single tests

Energy absorption

The results obtained from single impact tests allow for providing a benchmark for the sequential and multi-impact tests. A summery with these results in terms of velocities, energies and damage extension is shown in Table A.1 (see Appendix). The ballistic limit obtained for SCFR PEEK under the loading conditions applied was found V=195 m/s. The results in terms of residual velocity versus impact velocity curves obtained for SCFR PEEK are compared with experimental data of unfilled PEEK obtained by Garcia-Gonzalez et al. [16] in Fig. 4. These results were fitted via the expression proposed by Recht and Ipson [35]:

$$V_r = \left(V_0^k - V_{bl}^k\right)^{1/k} \quad (3)$$

where k is a fitting parameter with a value of 1.9 for both materials, and V_{bl} the ballistic limit. Comparing both materials, the residual velocity expected for a given impact velocity is lower

for unfilled PEEK, so that unfilled PEEK is able to absorb more energy for a given impact velocity.

In addition, the absorption energy capability of SCFR PEEK is shown in Fig. 5 by means of percentage of energy absorbed depending on the impact velocity. The composite material tested is able to absorb impact energies up to 32.5 J without perforation under the loading conditions imposed. Above this perforation threshold, a progressive decrease in the percentage of kinetic energy converted into work is observed, mainly governed by spalling failure mechanisms. Moreover, from impact energies of 120 J and higher (corresponding to impact velocities of 360 m/s), the percentage of absorbed energy decreases asymptotically to 25%.

Failure mode and time evolution

For velocities below the ballistic limit, the plate absorbs all the energy of the projectile mainly in form of matrix cracking damage. A localised ductile damage is observed in the first step of the impact process when the projectile impacts on the target, with a posterior creation of radial cracks. Low velocity impact involves a longer contact between impactor and the target. In addition, when impact velocity increases, the impact energy leads to a greater bending, which produces damage in regions far from the contact area (global structure deformation and bending), see Fig. 6. On the other hand, if the impact velocity of the projectile is enough to perforate the plate, part of the energy is absorbed by fibre cracking, fibre pull-out and local matrix failure (to create the plug), and other part of the energy is used to accelerate the plug (linear momentum transfer), Fig. 6. When the impact velocity increases (above ballistic limit), the damage is more localised around the impact zone resulting in a pull-out area that approaches the diameter of the projectile.

Finally, these results in terms of damage area are shown depending on the initial impact velocity in Fig. 7. Having into account that the active area of the plates is 10000 mm^2, the damage area increases with impact velocity until reaching 66% of the total extension at the ballistic limit and,

then, decreases until reaching an extension equal to the contact area between the projectile and the target.

3.3. Sequential tests

Energy absorption

The results in terms of velocities, energies and damage extension are collected in Table A.1 (Appendix), following the sequence: A the impact in the centre, B on the right and C on the left of the target). In the case of sequential test, the interaction of the second and third impacts with the previous radial cracks produces that impacts at velocities below the ballistic limit defined by single tests, result in the perforation of the plate. This is especially important when previous global damage have been observed. In Fig. 8, the absorbed energy for different impact conditions is shown for the first, second and third subsequent impacts. A reduction of the ballistic limit is obtained for the second and third impacts, 63% and 77% respectively. In addition, a lower energy absorption capability is observed for the second and third impacts at impact energies close to the ballistic limit with global damage. This difference in energy absorption is progressively reduced with an increase in impact energy due to a transition to local damage. Note that due to the overall extension of the damage area of the specimen tested at 195 m/s, a second and third impacts were not developed.

Failure mode and time evolution

The sequential tests aim at identifying the influence of previous damage on the mechanical response of the composite studied. To this end, these tests should be understood as sequential single impacts where the boundary and initial conditions of the specimen vary according to the previous loading, but do not take into account potential synergetic effects arising from stress waves interaction. The distance between impacts was greater than twice the diameter of the projectile. For impact velocities higher enough than the ballistic limit, the damage is localised at the impact region and no influence of this is observed in subsequent impacts. However, at velocities below and near the ballistic limit, an interaction with previous damage was observed for subsequent impacts, Fig. 9. In this case, due to previous damage of the first and second

impacts, the third one produces the detachment of a big area limited by radial cracks from the previous shots. This can be also observed in Fig. 10a where the cumulative damage area of the plate versus the mean impact velocity of the three impacts is represented. Note that while the damage between the first and subsequent impacts considerably differs for impact velocities close to the ballistic limit, this difference is significantly reduced for higher velocities when the damage per projectile becomes almost local.

3.4. Simultaneous impact tests

Energy absorption

The experimental results in terms of velocities, energies and damage extension for simultaneous impact tests are shown in Table A.2 (Appendix). Due to the pressure limits of the device used, the highest initial impact velocity reached was 250 m/s. In such experiments, although the impact velocity was the same for all projectiles, the residual velocities differed depending on the impact zone and on the combination of stress wave interaction and bending. The residual velocities of each projectile for different tests are shown in Table A.2 as: the first value is related to the impact on the left side of the plate; the second to the centre; the third to the right side. Note that the residual velocities obtained for an impact velocity of 151.8 m/s differ a lot between the three projectiles. This is explained by the fact that one projectile reaches the target considerably sooner than the other two, inducing a previous damage that, in combination with the stress waves interaction, help the subsequent projectiles to perforate the target easily. As for the single impacts, a decrease in the damage area is observed as the impact velocity increases, where a transition from global to local damage is also experienced. This transition with impact velocity is shown in Fig. 11. Moreover, when comparing the percentage of absorbed energy between single and the average results from simultaneous impact, there is a decrease in this percentage for the later due to synergetic effects, see Fig. 12.

Failure mode and time evolution

The simultaneous tests aim to show the influence of potential synergetic effects arising from stress waves interaction. The distance between impacts was measure using the grid drawn on the

samples. While with an initial velocity of 184.5 and 151.8 m/s the distance between impacts were around 1.25-1.5 cm, with an initial velocity of 131.2 and 249.42 m/s the distances were around 2-2.5 cm. Contrary to the sequential test where different damage area and failure mode were observed depending on if velocities were below or above the ballistic limit, a decrease in damage area was observed as impact velocity decreases Fig. 10b. This reduction in damage area results in a transition from a global to local damage.

4. Discussion

The use of thermoplastic composites in industrial applications that are exposed to impact loading makes the guarantee of their structural integrity against impact essential. As shown in the previous section, the mechanical response of SCFR PEEK components strongly depends on the loading conditions and potential previous damage. The impact process is likely to be caused by various projectiles/impactors hitting the structure both sequentially and simultaneously. With the aim of elucidating the influence of these loading conditions, single, sequential and simultaneous impact tests are presented in the previous section and discussed here.

The response of materials and structures to impulsive loading is quite complex. In this regard, the proper understanding of stress waves propagation and effects, along with local deformation and bending, is essential to understand the different fracture mechanisms. The stress waves that propagate through the material, as long as its yield point is not exceeded, are called elastic waves. Among them, the two principal waves are the longitudinal and the transverse waves [36]. In the longitudinal wave, which is also called primary P or dilatational wave, the particle motion is parallel to propagation the direction of the pulse and the strain is purely dilatational [37]. In the transverse wave, which is also called shear or distortional wave, the particle motion is normal to the propagation direction of the pulse and the strain is purely shearing [37]. The expressions of the longitudinal (c_L) and transverse waves speeds (c_S) read as:

$$c_L = \sqrt{\frac{K + \frac{4}{3}\mu}{\rho}} \tag{4}$$

$$c_S = \sqrt{\frac{\mu}{\rho}} \tag{5}$$

where ρ, K and μ are the density, the bulk modulus and the shear modulus of the material, respectively. The values of wave speeds for SCFR PEEK are $c_L \approx 2173\ m/s$ and $c_s \approx 4997\ m/s$.

In impact scenarios, a compressive pulse is propagated from the contact region until reaching a free surface, when the wave is reflected as a tensile wave. If the magnitude of this tensile wave is greater than the tensile strength of the material, brittle fracture occurs [37]. Moreover, if the magnitude of the stress pulse still exceeds the tensile strength value, multiple fractures can be observed [37]. In parallel to the longitudinal wave, a transverse wave propagates through the material carrying the shear pulse. This shear wave, along with local shear deformation, can lead to plastic flow if the intensity of the load is high enough to overcome the yield stress. If the yield stress is reached, plastic waves are present together with the elastic waves and a ductile fracture addressed by plastic flow is expected. In this regard, brittle fracture and plastic flow are assumed to be independent processes [38,39], where the tensile component of stress is responsible for brittle failure while ductile yielding occurs because of the influence of shear stress. Therefore, the failure mode is determined by which of these two stress thresholds, tensile strength or yield stress, is first overcome [39,40].

4.1. Discussion on single impact

As stated in previous section, the analysis in terms of damage extension shows two failure mechanisms regions: a first one for impact velocities bellow the ballistic limit; and a second one above the ballistic limit. In Fig. 13, the different damage mechanics are represented depending on the initial impact velocity, being the first row the front part of the specimens and the second row the rear part. During the impacts that do not reach the ballistic limit, the target plate absorbs the whole kinematic energy of the projectile by elastic mechanisms and dissipative ones resulting in cracking damage of the matrix (Fig. 13a and 13b). In the transition region corresponding to close impact velocities to the ballistic limit, a local damage in the impact region is propagated in form of cracking covering almost the whole active area of the plate, thus leading to a global damage in the specimen tested (Fig. 13c). A localised ductile damage is observed in the first step of the impact event due to shear stress. Due to the impact process, a

train of compression pulses propagates through the specimen and reflects as a train of tensile waves that, along with tension from bending, can result in a circumferential brittle failure. If the specimens impacted are further analysed, we realised that the radial cracks that propagate through the rear surface cover bigger extensions than in the front surface (Fig. 13).
This fact finds explanation in the lower tensile strength in comparison with the compressive value. As the initial impact velocity increases, a transition from local to global damage is observed where circumferential cracks are also formed. Moreover, when the impact velocity is higher than the ballistic limit, another transition from global to local damage is experienced (Fig. 13d, 13e and 13f). In addition, an increase in impact velocity above the ballistic limit favours the failure of the specimen by spalling as result of the reflection of the initial compressive wave and, at even higher velocities, by plugging. This spall surface becomes smaller with impact velocity as well as the extension of the radial cracks (until the no presence of cracks above a critical impact velocity), see Fig. 13e and 13f. A scheme with the different damage mechanisms depending on impact velocity is presented from the single impact tests conducted in Fig. 14.

4.2. Discussion on sequential impact

The final stage of SCFR PEEK plates after three sequential impacts is presented in Fig. 15 for: low impact velocity regime (Fig. 15a); transition regime at close impact velocities to the ballistic limit for single impact (Fig. 15b); high velocity regime (Fig. 15c). The upper row in Fig. 15 corresponds with the front part of the specimens and the lower row with the rear part. The same failure mechanisms described for single tests were observed. However, the interaction between cracks plays a crucial role that is necessary to take into account. For the low impact velocity regime, the specimen is capable to support the three sequential impacts without penetration. However, the cracks that propagate from the impact region interact leading to higher damage extension than the expected from single tests. This crack interaction becomes more important with impact velocity increase, resulting in the collapse of the material and, subsequently, in projectile penetration at velocities considerably lower than the ballistic limit

found for single test (160 m/s in Fig. 15b). From the analysis of the damage extension, the cracks associated to the first impact were found to determine the failure pathways induced by the second and third impacts, Fig. 15b. On the contrary, for the high impact velocity regime, the damage extension is much localised at the impact region without showing secondary failure mechanisms by means of crack propagation. This localised damage translates into no influence of the first impact on the subsequent ones (Fig. 15c).

When the energy absorption capability of the material is compared within the sequential tests, a reduction for the second and third impacts is observed, see Fig. 8. Therefore, for impact energies that overpass the elastic response of the composite behaviour, an accumulative inelastic deformation is observed on the plate in the form of plastic deformation or cracking-based failure after the first impact. Then, when a second projectile reaches the target, different things can happen:

(i) The second projectile impacts on a damaged region or induces cracking propagation reaching a damaged region (Fig. 15a and 15b). Here, the effects of this impact are more damaging than an equivalent single test. This higher damage is explained by the energy absorption in this zone of the plate, which is mainly dissipated by inelastic mechanisms leading to permanent deformation that increases the damage extension within the specimen.

(ii) The impact velocity is high enough ($V_0 >> V_{bl}$) to induce a fully localised damage without affecting the previous affected region (Fig. 15c). In such scenario, the consequences of subsequent impacts can be assumed equivalent as a single test.

4.3. Discussion on simultaneous impact effects

The sequential tests analysis suggests the potential relevance of considering simultaneous impacts where the interaction between stress waves, tension from bending and cracks may play a decisive role. To this end, the configuration chosen for the sabot ensures a distance between impacts greater than twice the projectile diameter to avoid the interaction of local effects. The final stage of SCFR PEEK plates after three simultaneous impacts is presented in Fig. 16 for different impact velocities. The upper row corresponds with the front side of the specimens and

the lower row with the rear side. As with the sequential impacts, different scenarios can happen depending on the impact velocity:

(i) At low impact velocities (less than 140 m/s), cracks from the three impacted regions propagate interacting between them and resulting in higher damage extent (global damage region). In addition, the simultaneous impacts induces higher bending that results in concentration of tensile stress and the subsequent circumferentially brittle fracture.

(ii) At impact velocities above 140 m/s and below the ballistic limit for single test, there is a transition from global to local damage that is mainly governed by brittle fracture arising from tensile stress related to bending along with reflected stress waves.

(iii) At enough high impact velocities ($V_0 >> V_{bl}$), the projectiles perforate the specimen locally and push plugs out of the target with an extension of approximately the diameter of the projectile. However, the interaction between stress waves and local bending can result in some cracks between impact regions.

5. Conclusions

In this work, the impact mechanical behaviour of SFR thermoplastics was deeply investigated against single and multiple impacts. To this end, SCFR PEEK was selected as baseline material due to its current and increasing employment in a wide variety of industrial applications. The mechanical impact response of this composite was tested first against single impact and, then, against sequential and simultaneous impacts to elucidate the effects of previous damage in the specimen and stress wave interactions along with tensile stress from bending. The principal results obtained in this work can be synthesised as:

- The ballistic limit from single test cannot be extrapolated to sequential and simultaneous tests.
- Sequential tests showed a reduction in the ballistic limit when a second or subsequent projectile impacts the target. The second impact can affect the previous damaged region by direct contact or through the propagation of its associated cracks, resulting in the catastrophic failure of the material. Moreover, this can occur even if the second impact does not take place on the previous damaged region. In this regard, the stress waves transmitted along the structure can reach the damaged region leading to structural collapse.
- Simultaneous impact tests showed a reduction in the ballistic limit with respect to single impact. In addition, the combined effects of the interaction between cracks propagation, stress waves (especially the reflected tensile waves) and complex bending effects (leading to high local tensile stress) is observed to govern the fracture mechanisms and the damage extent.

The results presented in this work conclude that the study of the mechanical impact behaviour of SFR thermoplastics must address scenarios that consider more than only one projectile. This aspect is essential since most of the real impact scenarios involve various projectiles/impactors impacting sequentially of simultaneously. While single impact testing faithfully provides the main deformation and failure mechanisms of the material under impact loading, it does not provide reliable predictions of its in-service mechanical response. As key conclusion, multi-

impact tests are necessary to guarantee the structural response of composite structures potentially subjected to such scenarios.

Acknowledgements

The researchers are indebted to Ministerio de Economía y Competitividad de España (Project DPI2014-57989-P) and Vicerrectorado de Política Científica UC3M (Project 2013-00219-002) for financial support. The researchers are indebted to LATI Company for PEEK material supplied. The authors express their thanks to Mr. Sergio Puerta, Mr. David Pedroche for their technical support.

References

1 Rae P, Brown E, Orler E. The mechanical properties of poly(ether-ether-ketone) (PEEK) with emphasis on the large compressive strain response. Polymer 2007;48:598–615.

2 Garcia-Gonzalez D, Zaera R, Arias A. A hyperelastic-thermoviscoplastic constitutive model for semi-crystalline polymers: application to PEEK under dynamic loading conditions. Int J Plast 2017a;88:27–52.

3 Garcia-Gonzalez D, Garzon-Hernandez S, Arias A. A new constitutive model for polymeric matrices: Application to biomedical materials. Compos Part B 2018;139-117-129.

4 Rezaei R, Yunus R, Ibrahim N. Effect of fiber length on thermomechanical properties of short carbon fiber reinforced polypropylene composites. Mater Des 2009;30:260–3.

5 Garcia-Gonzalez D, Rodriguez-Millan M, Rusinek A, Arias A. Low temperature effect on impact energy absorption capability of PEEK composites. Compos Struct 2015a;134:440–9.

6 Garcia-Gonzalez D, Rusinek A, Jankowiak T, Arias A. Mechanical impact behavior of polyether–ether–ketone (PEEK). Compos Struct 2015b;124:88-99.

7 Scholz MS, Blanchfield JP, Bloom LD, Coburn BH, Elkington M, Fuller JD, et al. The use of composite materials in modern orthopaedic medicine and prosthetic devices: a review. Compos Sci Technol 2011;71(16):1791-803.

8 Lovald S, Kurtz S. Applications of polyetheretherketone in trauma, arthroscopy and cranial defect repair. In: Kurtz S, editor. PEEK biomaterials handbook. William Andrew Elsevier; 2012. p. 243–60.

9 Ramsteiner F, Theysohn R. Tensile and impact strengths of unidirectional. Short Fiber-Reinf Thermoplast Compos 1979;10:111–9.

10 Sarasua JR, Remiro PM, Pouyet J. The mechanical behaviour of PEEK short fibre composites. J Mater Sci 1995;30(13):3501-8.

11 Garcia-Gonzalez D, Jayamohan J, Sotiropoulos N, Yoon H, Cook H, Siviour C, et al. On the mechanical behaviour of PEEK and HA cranial implants under impact loading. J Mech Behav Biomater 2017b;69:342–54.

12 Cantwell WJ, Morton J. Comparison of the low and high velocity impact response of CFRP. Composites, 1989, 20(6), 545–551.

13 Arias A, Rodríguez-Martínez JA, Rusinek A. Numerical simulations of impact behaviour of thin steel plates subjected to cylindrical, conical and hemispherical non-deformable projectiles. Eng Fract Mech 2008;5:1635–56.

14 Rodríguez-Martínez JA, Pesci R, Rusinek A, Arias A, Zaera, R. Thermo-mechanical behaviour of TRIP 1000 steel sheets subjected to low velocity perforation by conical projectiles at different temperatures. Int J Sol Structures 2010; 47(9):1268-1284.

15 Rodriguez-Millan M, Vaz-Romero A, Rusinek A, Rodriguez-Martinez J, Arias A. Experimental Study on the Perforation Process of 5754-H111 and 6082-T6 Aluminium Plates Subjected to Normal Impact by Conical, Hemispherical and Blunt Projectiles. Exp Mech 2014;54:729-742.

16 Garcia-Gonzalez D, Rodriguez-Millan M, Rusinek A, Arias A. Investigation of mechanical impact behavior of short carbon-fiber-reinforced PEEK composites. Compos Struct 2015c;133:1116–26.

17 Bartus S. Simultaneous and sequential multi-site impact response of composite laminates. 2006. In: Phd Thesis. University of Alabama at Birmingham

18 Russel B. Multi-hit ballistic damage characterisation of 304 stainless steel plates with finite elements. Mater Design 2014; 58:252-264.

19 Amaro A, Reis P, Moura M, Neto M. Influence of multi-impacts on GRP composite Laminates. Compos Part B 2013; 52;93-99.

20 Green S. Chapter 3 – Compounds and composite materials. In: PEEK biomaterials handbook. William Andrew Elsevier; 2012. p. 23–48.

21 Borruto A. A new material for hip prosthesis without considerable debris release. Med Eng Phys 2010;32:908–13.

22 Horsfall I, Austin S, Bishop W. Structural ballistic armour for transport aircraft. Mater Design 2000; 21:19-25.

23 Hazell P J, Roberson CJ, Moutinho M. The design of mosaic armour: the influence of tile size on ballistic performance. Mater Design 2008;29:1497-1503

24 Deka J, Bartus S, Vaidya U. Multi-site impact response of S2-glass/epoxy composite laminates. Compos Sci Tech 2009; 69(6); 725-735.

25 Lee, DJ. On studies of tensile properties in injection molded short carbon fiber reinforced PEEK composite. KSME Journal 1996;10:362-71

26 Rodríguez-Martínez JA, Rodríguez-Millán M, Rusinek A. A dislocation-based constitutive description for modeling the behavior of FCC metals within wide ranges of strain rate and temperature. Mechanics Maters 2011;43 (12): 901-912.

27 Bogetti TA, Walter M, Staniszewski J, Cline J. Interlaminar shear characterization of ultra-high molecular weight polyethylene (UHMWPE) composite laminates. Compos Part A-Appl S 2017;98:105–115.

28 Fu S-Y, Lauke B, Mai Y-W. Science and Engineering of Short Fibre Reinforced Polymer Composites. Extrusion compounding and injection moulding. 6-27. Woodhead Publishing. 6th July 2009.

29 Kammoun S, Doghri I, Adam L, Robert G, Delannay L. First pseudo-grain failure model for inelastic composites with misaligned short fibers. Compos Part A-Appl S 2011;42:1892–902

30 Steinberg EL, Rath E, Shlaifer A, Chechik O, Maman E, Salai M. Carbon fiber reinforced PEEK Optima—A composite material biomechanical properties and wear/debris characteristics of CF-PEEK composites for orthopedic trauma implants. J Mech Behav Biomed 2013;17:221–8.

31 Molazemhosseini A, Tourani H, Naimi-Jamal M, Khavand A. Nanoindentation and nanoscratching responses of PEEK based hybrid composites reinforced with short carbon fibers and nano-silica. Polym Test 2013;32:525–34.

32 Qian L, Qu M, Feng G. Study on terminal effects of dense fragment cluster impact on armor plate. Part I: Analytical model. Int J Impact Eng 2005; 31: 755-767.

33 Qian L, Qu M. Study on terminal effects of dense fragment cluster impact on armor plate. Part II: Numerical simulations. Int J Impact Eng 2005; 31: 769-780.

34 Kechagiadakis, G., Pirlot, M., "Development of a tool for testing PPE under near simultaneous Triple Impacts", 12th IARP WS HUDEM'2014, Zadar, Croatia, April 2014.

35 Recht RF, Ipson TW. Ballistic perforation dynamics. J Appl Mech 1963;30(3):384-90.

36 Meyers MA. Dynamic behavior of materials, 1994. Ed. John Wiley & Sons.

37 Zukas JA, Nicholas T, Swift HF, Greszczuk LB; Curran DR. Impac dynamics. Wiley;1992.

38 Orowan E .Fracture and strength of solids. Rep Prog Phys 1949;12:185-232.

39 Motz H, Schultz JM. Mechanical failure in PEEK and its short-fiber composites. J Thermoplast Compos 1990;3(2):110-30.

40 Chen C, Zhang C, Liu C, Miao Y, Li Y. Rate-dependent tensile failure behavior of short fiber reinforced PEEK. Compos Part B: Eng 2018, 136(1): 187-196.

FIGURE CAPTIONS

FIGURE 1

Fig. 1. Experimental device.

FIGURE 2

Fig. 2. Geometry of plate specimen and boundary conditions (dimensions in mm).

FIGURE 3

Fig. 3. Definition of damage area.

FIGURE 4

Fig. 4. Residual velocity V_r versus impact velocity V_0 for single impact tests on SCFR PEEK.

FIGURE 5

Fig. 5. Percentage of absorbed energy by SCFR PEEK versus impact energy.

FIGURE 6

Fig. 6. Failure stages of the impact process at impact velocities of: (upper) ballistic limit, 195 m/s; (lower) above ballistic limit, 463.6 m/s.

FIGURE 7

Fig. 7. Damage area of single impact versus impact velocity.

FIGURE 8

Fig. 8. Percentage of absorbed energy of SCFR PEEK versus impact energy, comparison between first, second and third impacts.

FIGURE 9

Fig. 9. Failure stages of the three-impact sequential test: (a) first impact at 168.3 m/s; (b) second impact at 167.6 m/s; (c) and (d) third impact at 159 m/s.

FIGURE 10

Fig. 10. Comparison of the damage area versus impact velocity between: (a) single and sequential impact tests; (b) sequential and simultaneous impact tests.

FIGURE 11

Fig. 11. Failure stages of the three-impact simultaneous test: (a) impact at 131.2 m/s; (b) impact at 249.4 m/s.

FIGURE 12

Fig. 12. Percentage of absorbed energy of SCFR PEEK versus impact energy, comparison between single impact and averages simultaneous impact.

FIGURE 13

Fig. 13. Final stage of single impact at different velocities (upper images show the front surface and lower images the rear surface): (a) 119.5 m/s; (b) 168.3 m/s; (c) 195 m/s; (d) 271 m/s; (e) 368.3 m/s; (f) 463.6 m/s

FIGURE 14

Fig. 14. Different damage mechanisms as a function of the impact velocity.

FIGURE 15

Fig. 15. Final stage of three sequential impacts at different velocities (upper images show the front surface and lower images the rear surface): (a) 107.5 m/s; (b) 165 m/s; (c) 469 m/s.

FIGURE 16

Fig. 16. Final stage of three simultaneous impacts at different velocities (upper images show the front surface and lower images the rear surface): (a) 131.2 m/s; (b) 151.8 m/s; (c) 184.5 m/s; (d) 249.4 m/s.

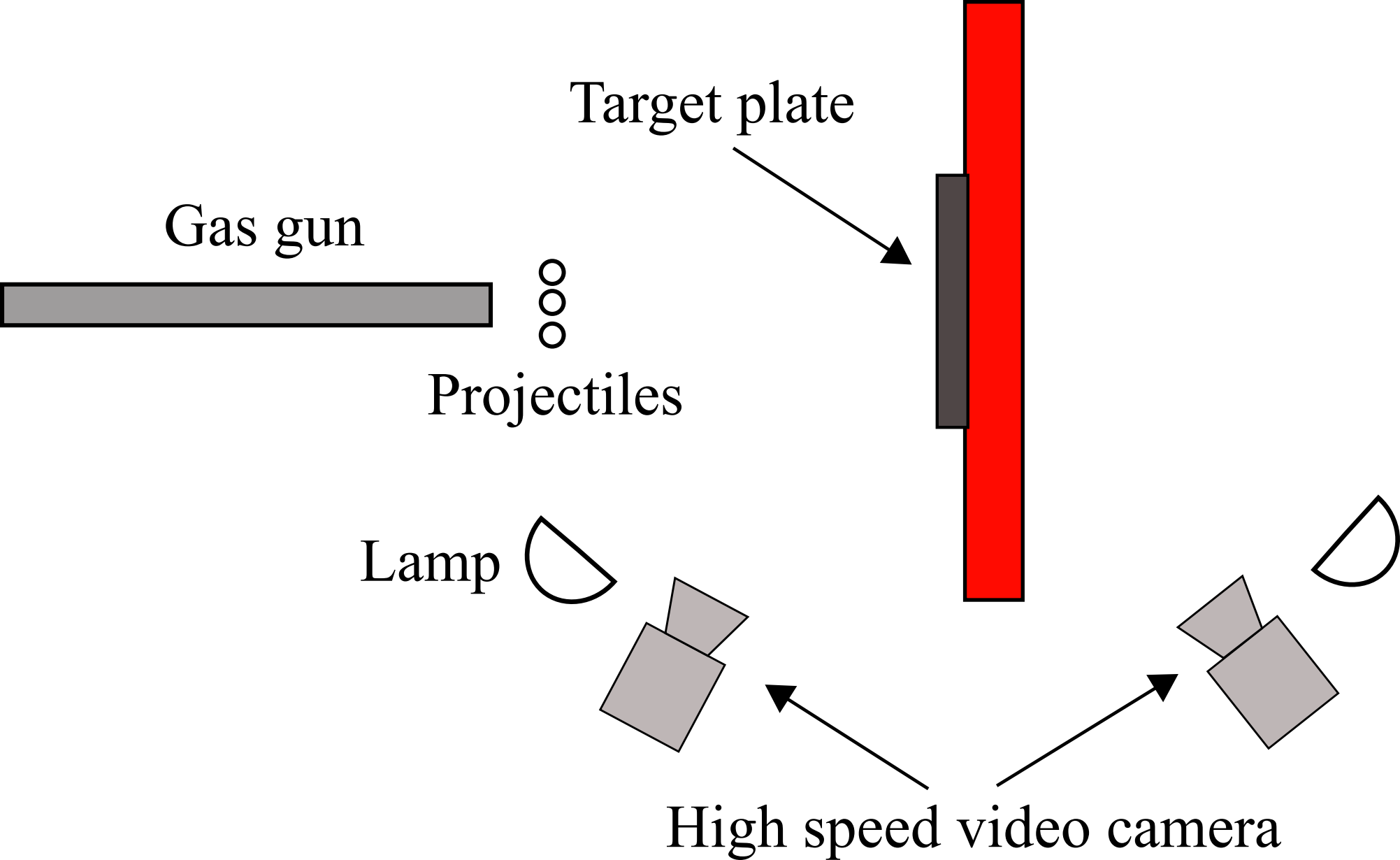
Target plate
Gas gun
Projectiles
Lamp
High speed video camera

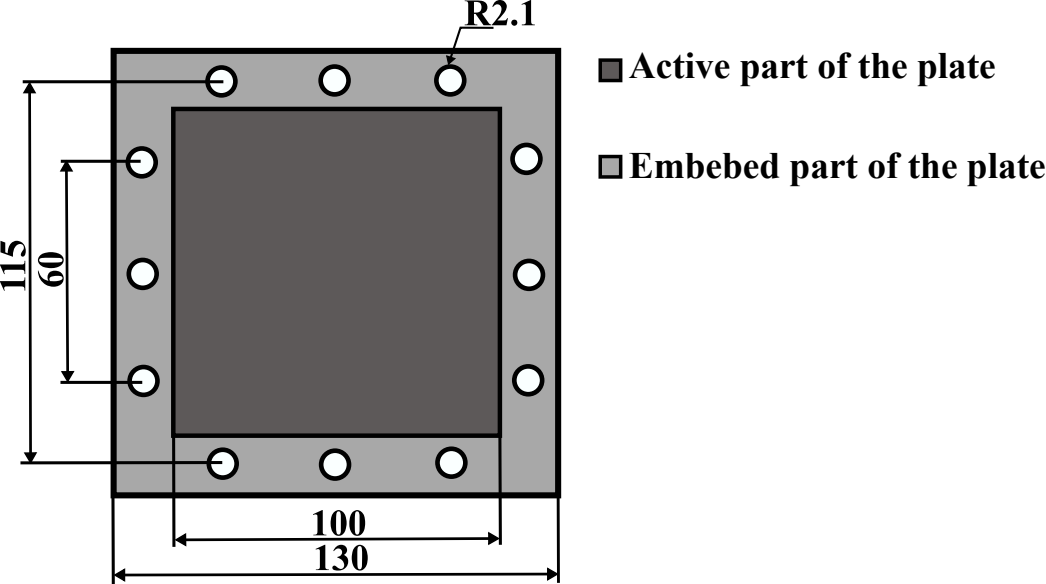
R2.1
Active part of the plate
Embebed part of the plate
115
60
100
130

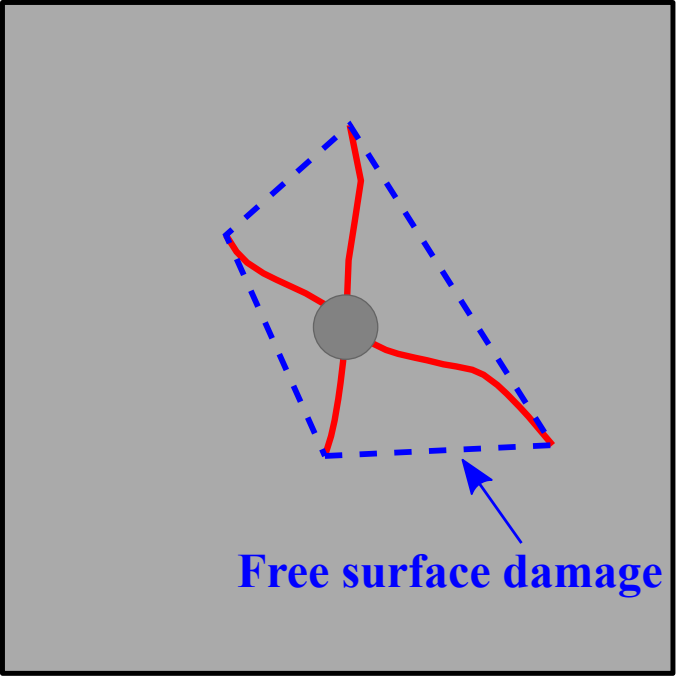

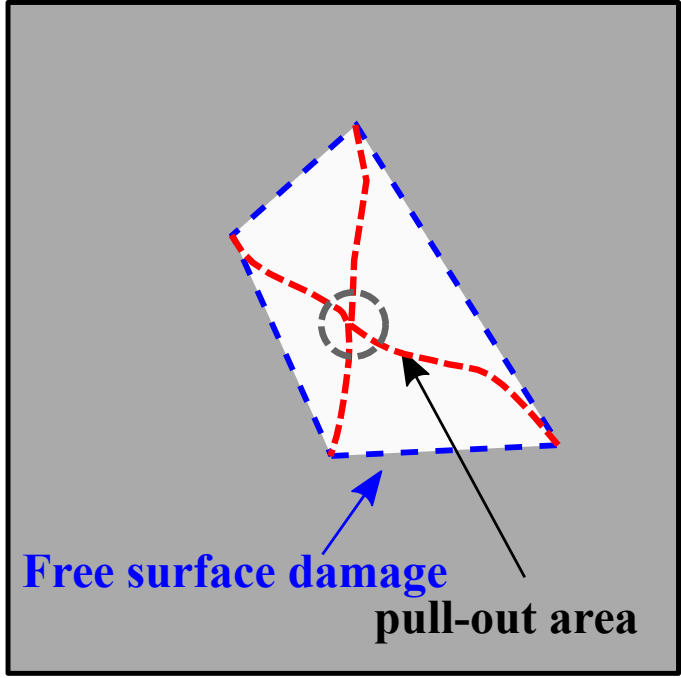

below balistic limit **above balistic limit**

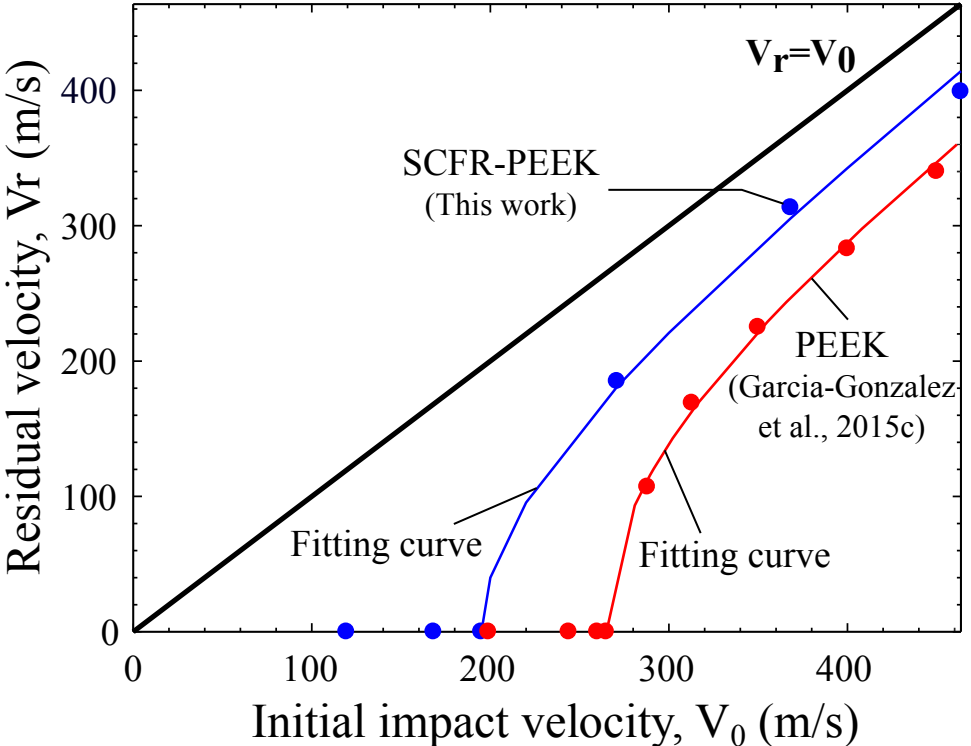
Residual velocity, Vr (m/s)
Initial impact velocity, V0 (m/s)
0
100
200
300
400
Vr=V0
SCFR-PEEK
(This work)
PEEK
(Garcia-Gonzalez-
et al., 2015c)
Fitting curve
Fitting curve

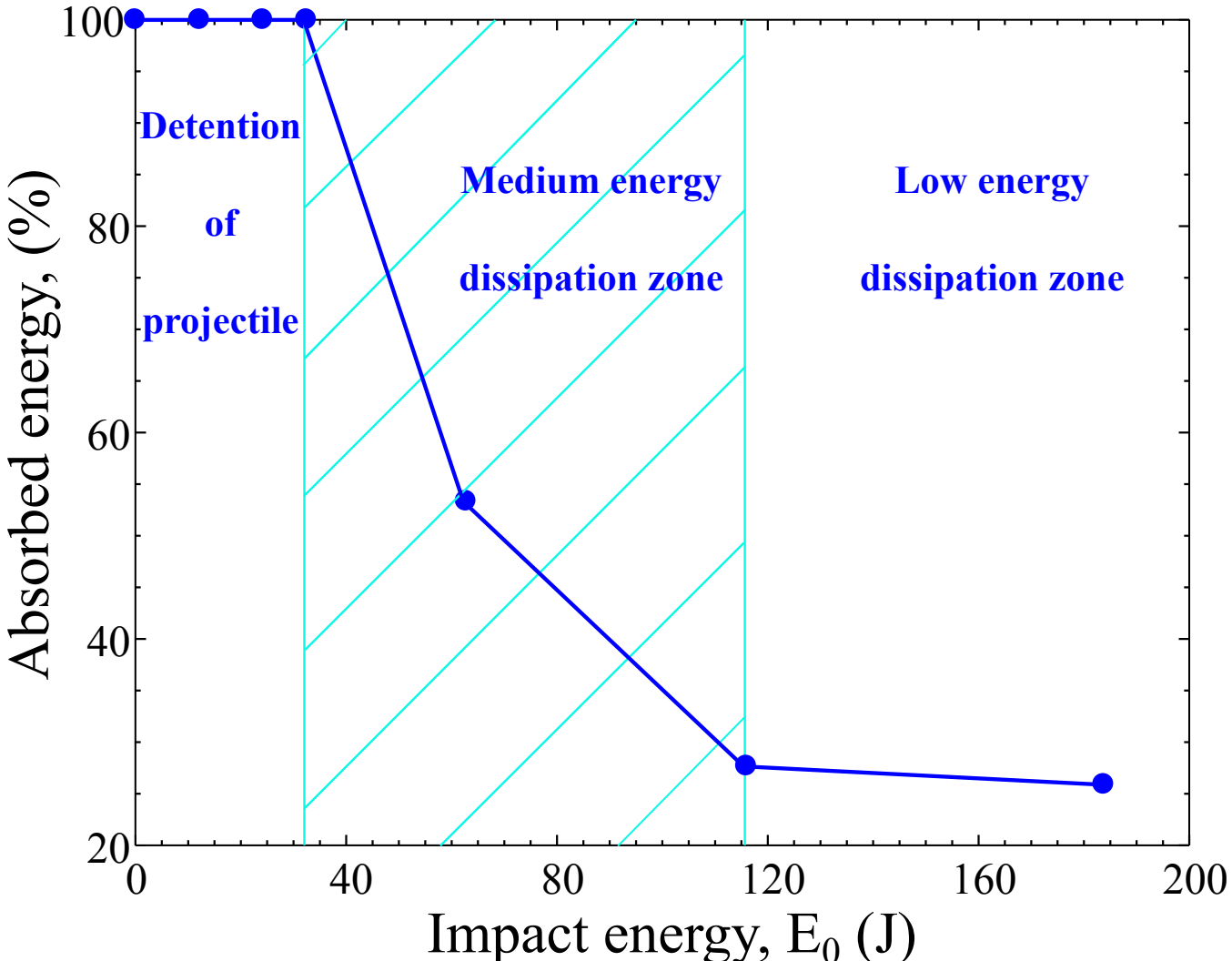
Detention
of
projectile
Medium energy
dissipation zone
Low energy
dissipation zone
Absorbed energy, (%)
100
80
60
40
20
0
40
80
120
160
200
Impact energy, E0 (J)

Ballistic limit

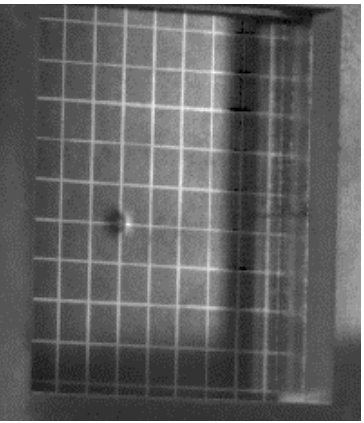

Contact of the projectile with the target (t=0 μs)

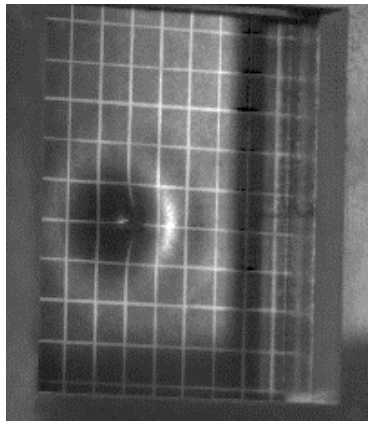

Iniciation of bending and cracks (t=20 μs)

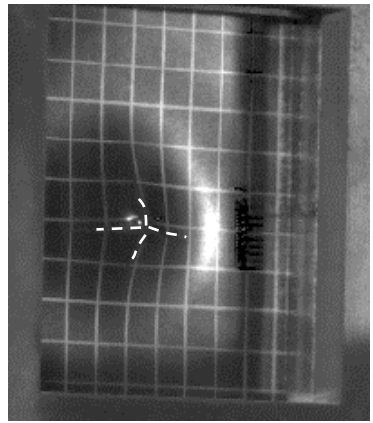

Cracks and bengind growth (t=60 μs)

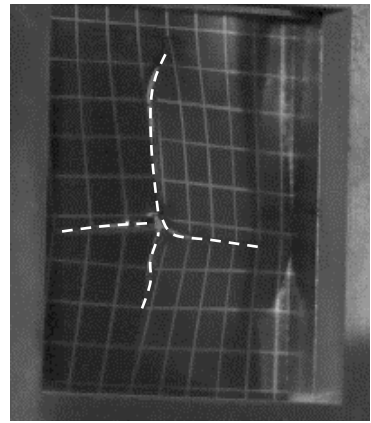

Global bending (t=390 μs)

Above ballistic limit

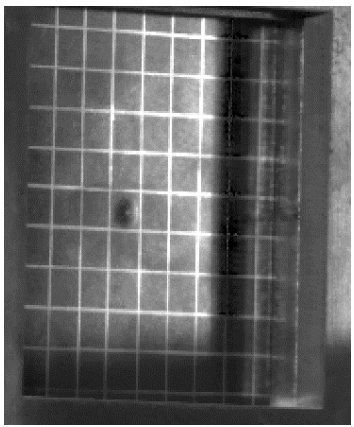

Contact of the projectile with the target (t=0 μs)

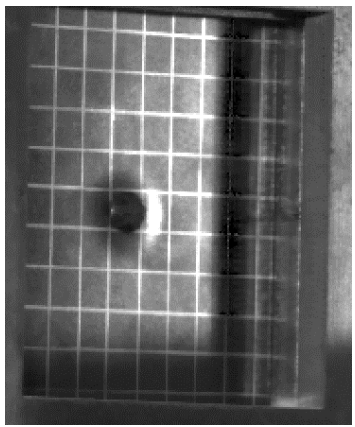

Iniciation of shear perforation (t=10 μs)

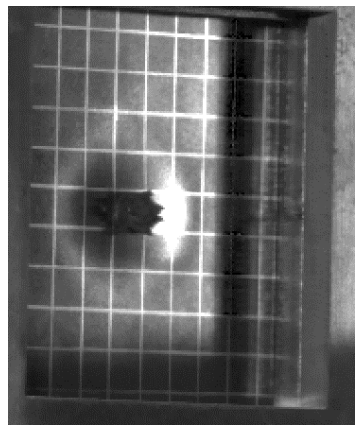

Local bending and initiation of plug (t=20 μs)

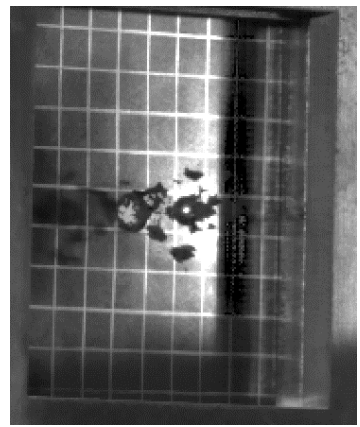

Perforation (t=70 μs)

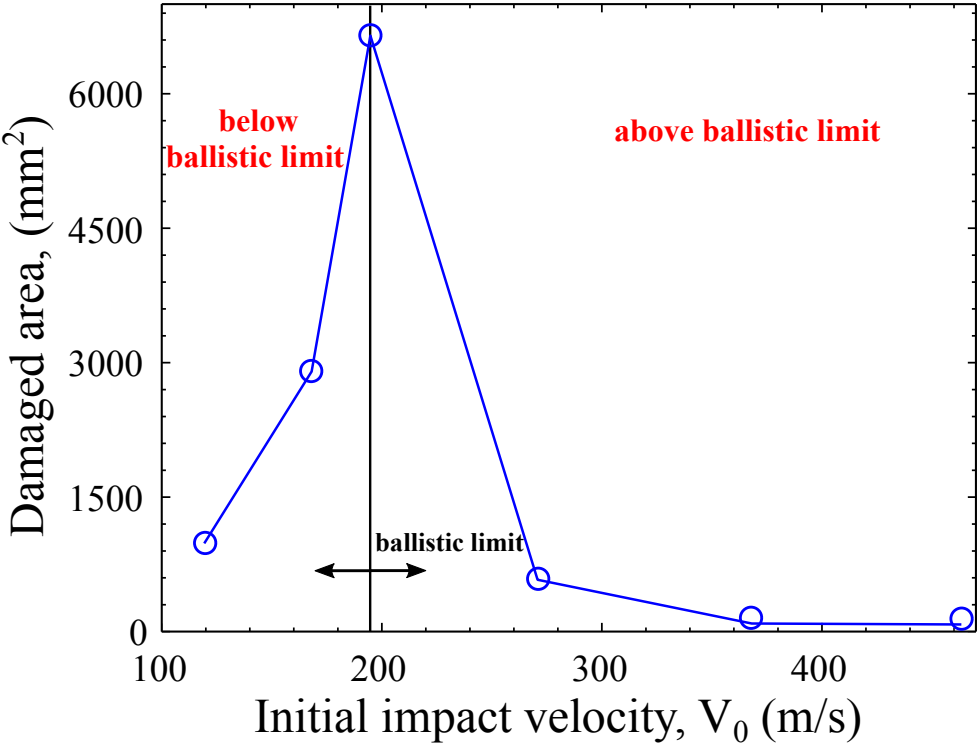
below
ballistic limit
above ballistic limit
ballistic limit
Damaged area, (mm^2)
6000
4500
3000
1500
0
100
200
300
400
Initial impact velocity, V_0 (m/s)

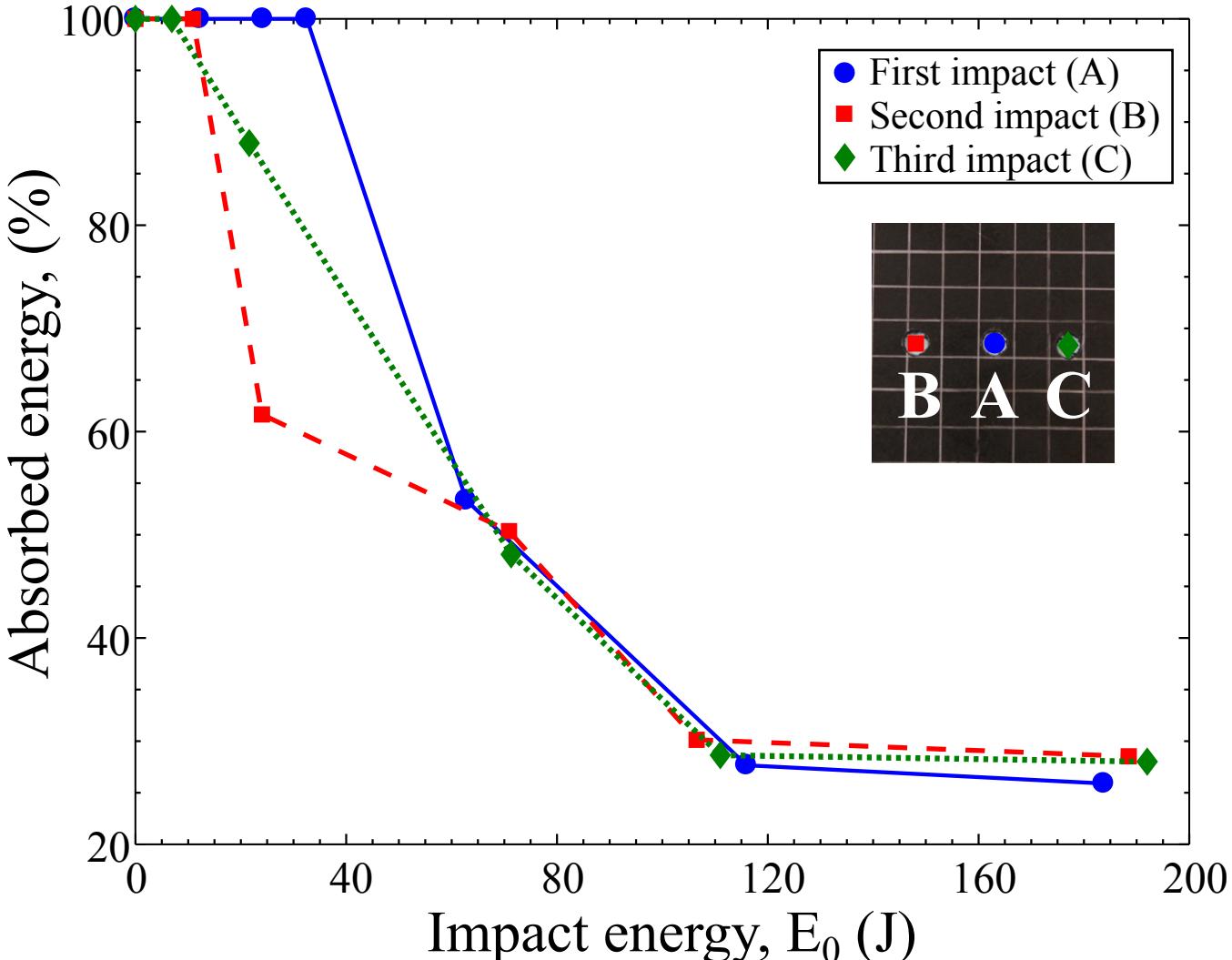
First impact (A)
Second impact (B)
Third impact (C)
B A C
Absorbed energy, (%)
100
80
60
40
20
0
40
80
120
160
200
Impact energy, E0 (J)

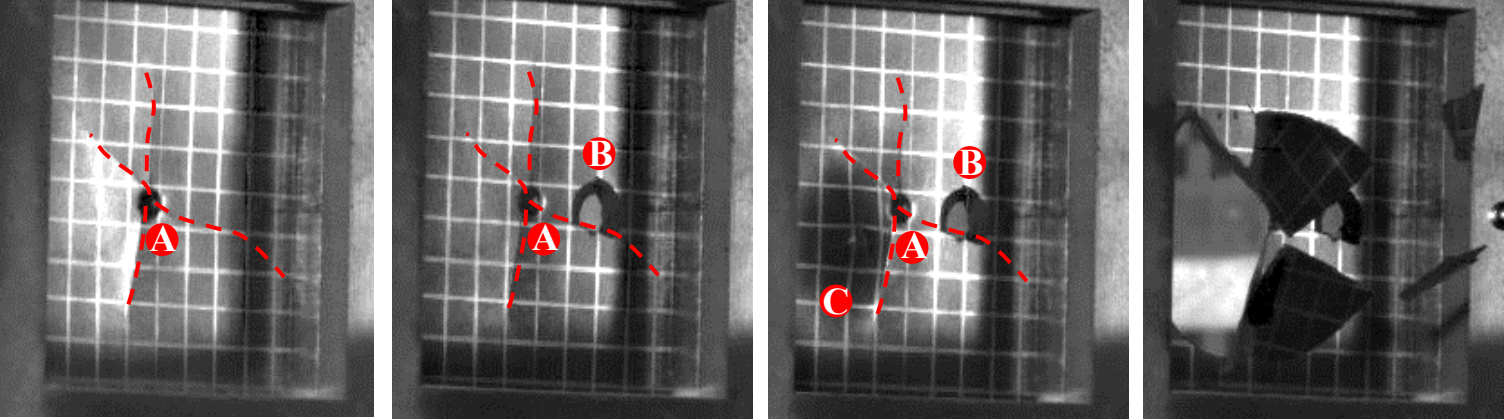

(a) (b) (c) (d)

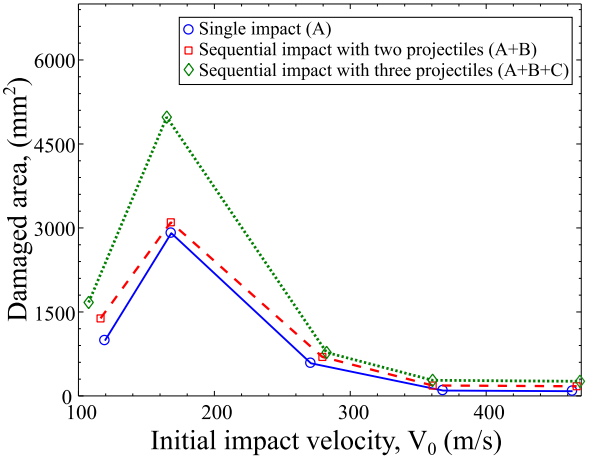
Single impact (A)
Sequential impact with two projectiles (A+B)
Sequential impact with three projectiles (A+B+C)
Damaged area, (mm^2)
Initial impact velocity, V_0 (m/s)
0
1500
3000
4500
6000
100
200
300
400

(a)

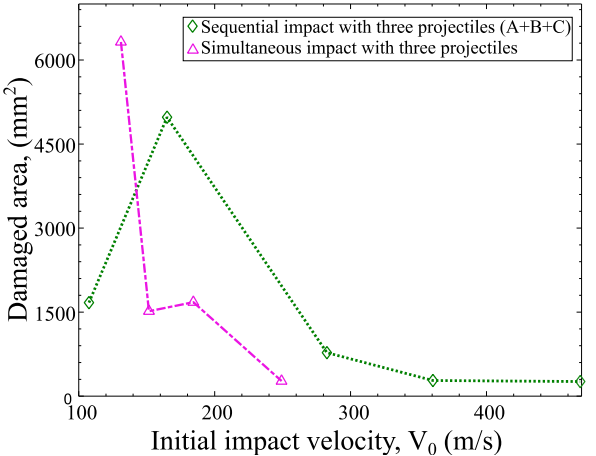
Sequential impact with three projectiles (A+B+C)
Simultaneous impact with three projectiles
Damaged area, (mm^2)
Initial impact velocity, V_0 (m/s)
0
1500
3000
4500
6000
100
200
300
400

(b)

V_0 =131.2 m/s

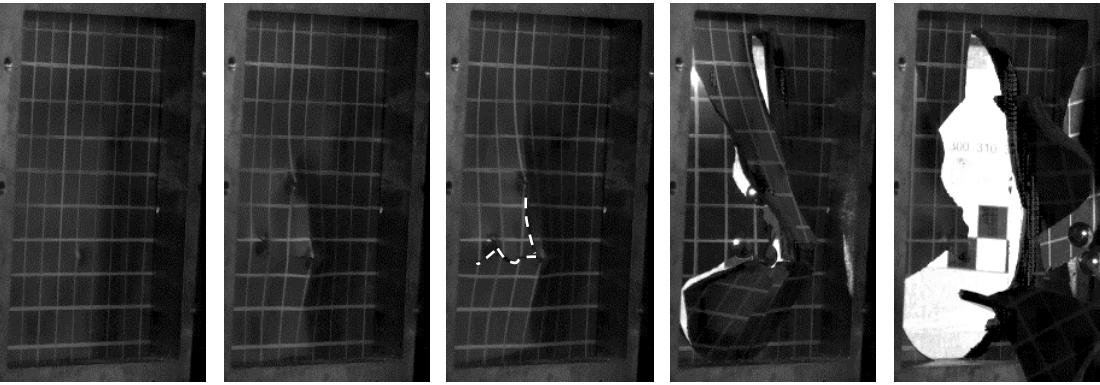

t=0 μs t=57μs t=100 μs t=443μs t=2628 μs

V_0 =249.4 m/s

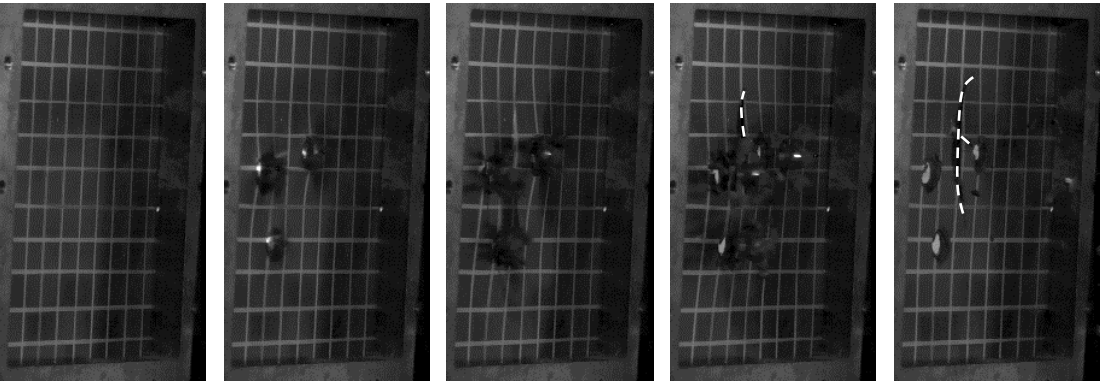

t=0 μs t=29μs t=57μs t=86 μs t=543 μs

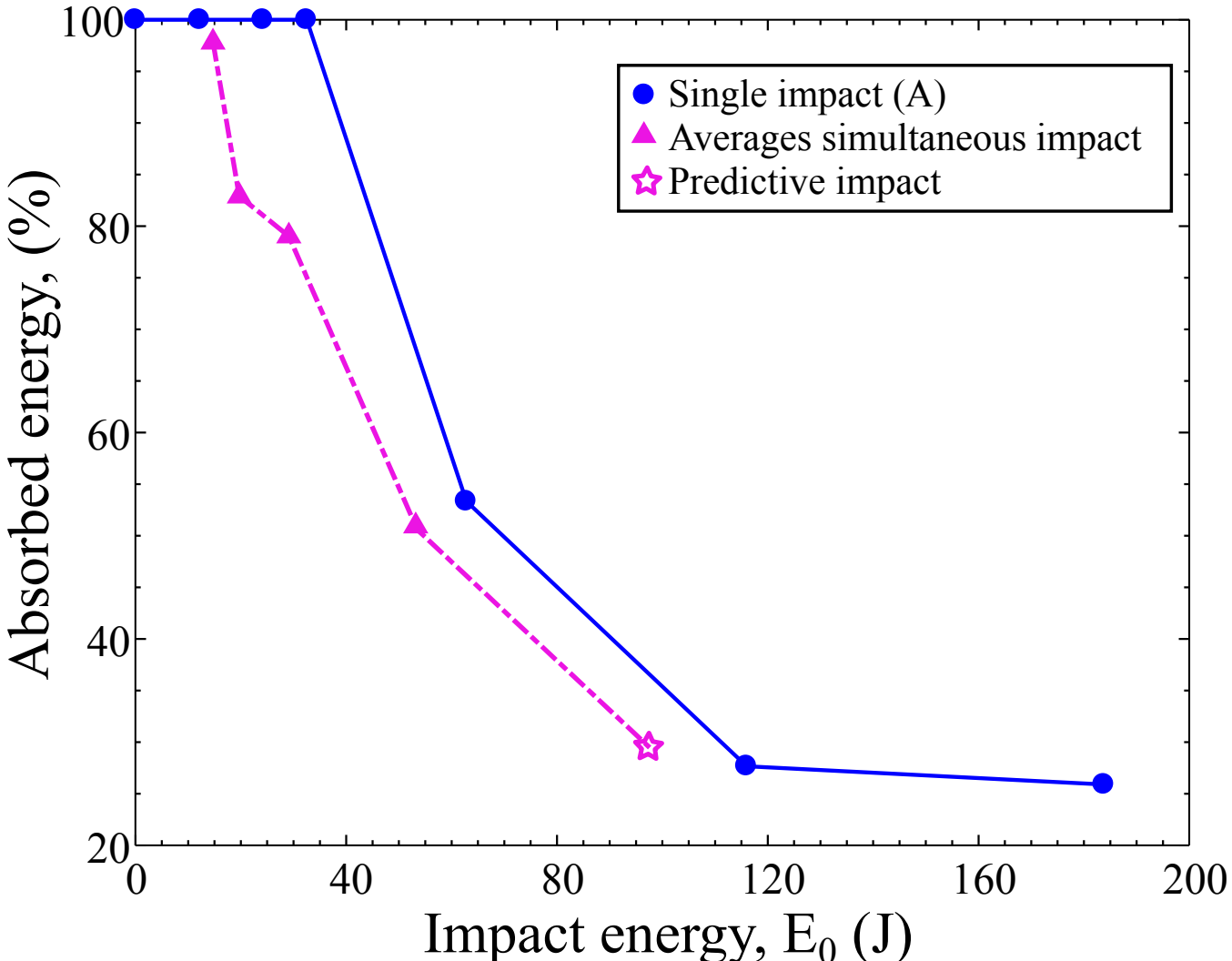
Single impact (A)
Averages simultaneous impact
Predictive impact
Absorbed energy, (%)
Impact energy, E0 (J)
100
80
60
40
20
0
40
80
120
160
200

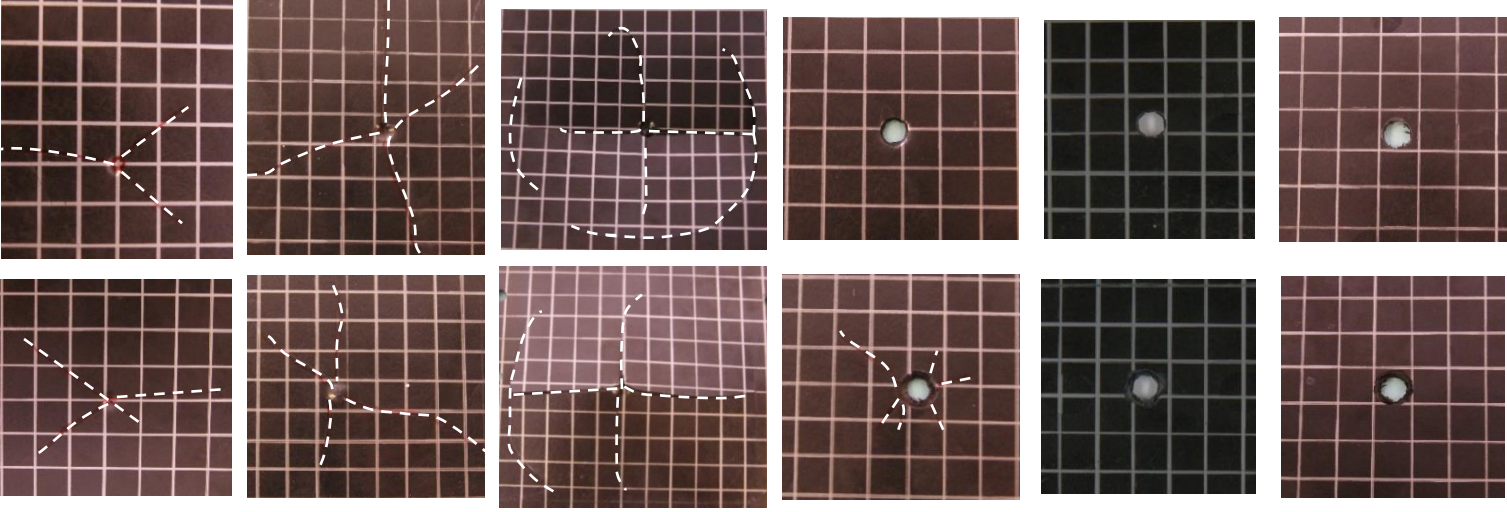
Impact velocity increase
(a)
(b)
(c)
(d)
(e)
(f)

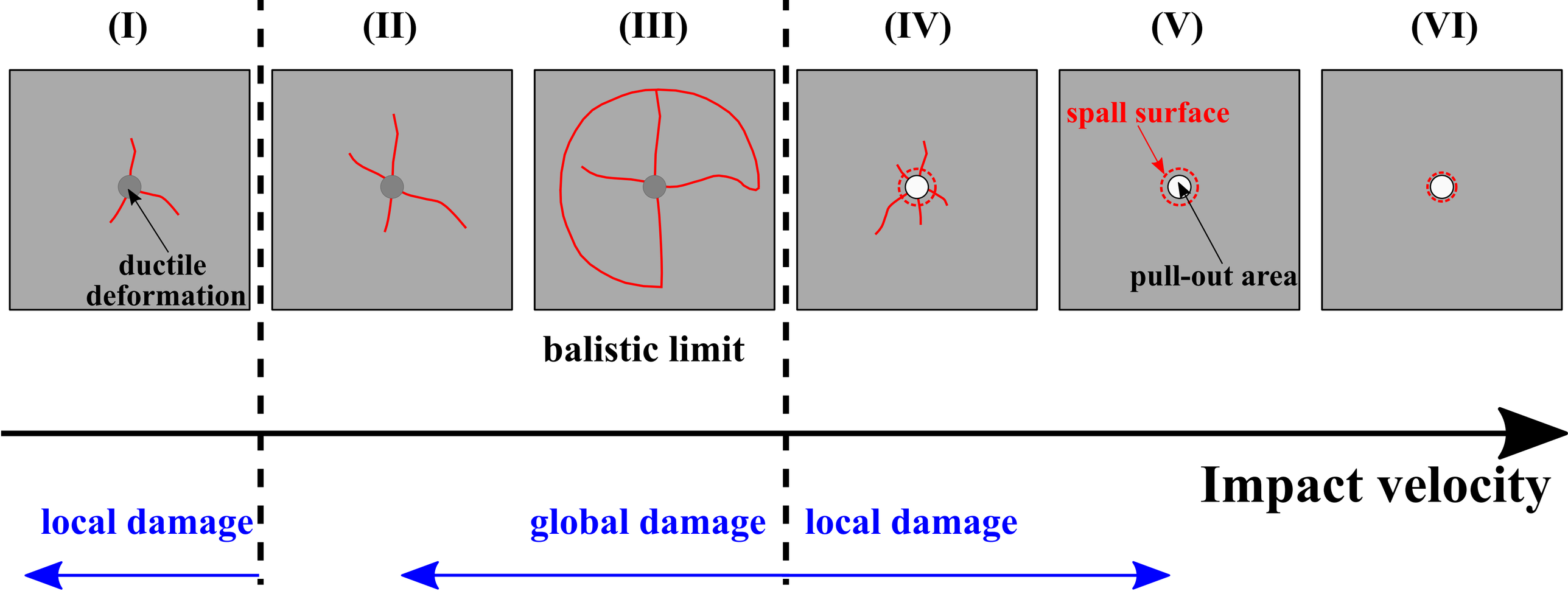
(I)
(II)
(III)
(IV)
(V)
(VI)
ductile deformation
spall surface
pull-out area
balistic limit
Impact velocity
local damage
global damage
local damage

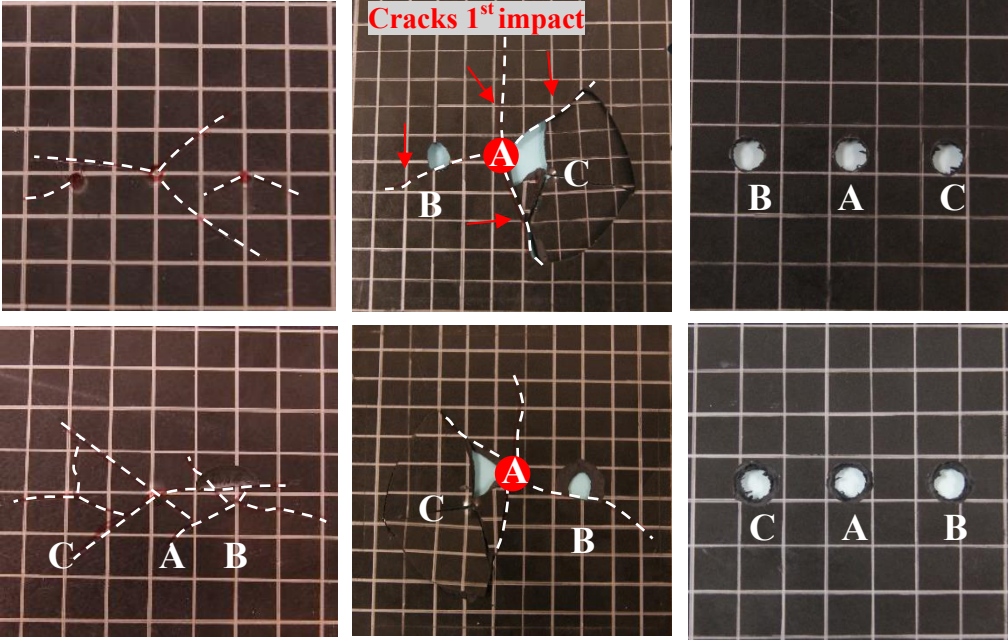
Cracks 1st impact
A
B
C
B
A
C
C
A
B
A
C
B
C
A
B
Impact velocity increase
(a)
(b)
(c)

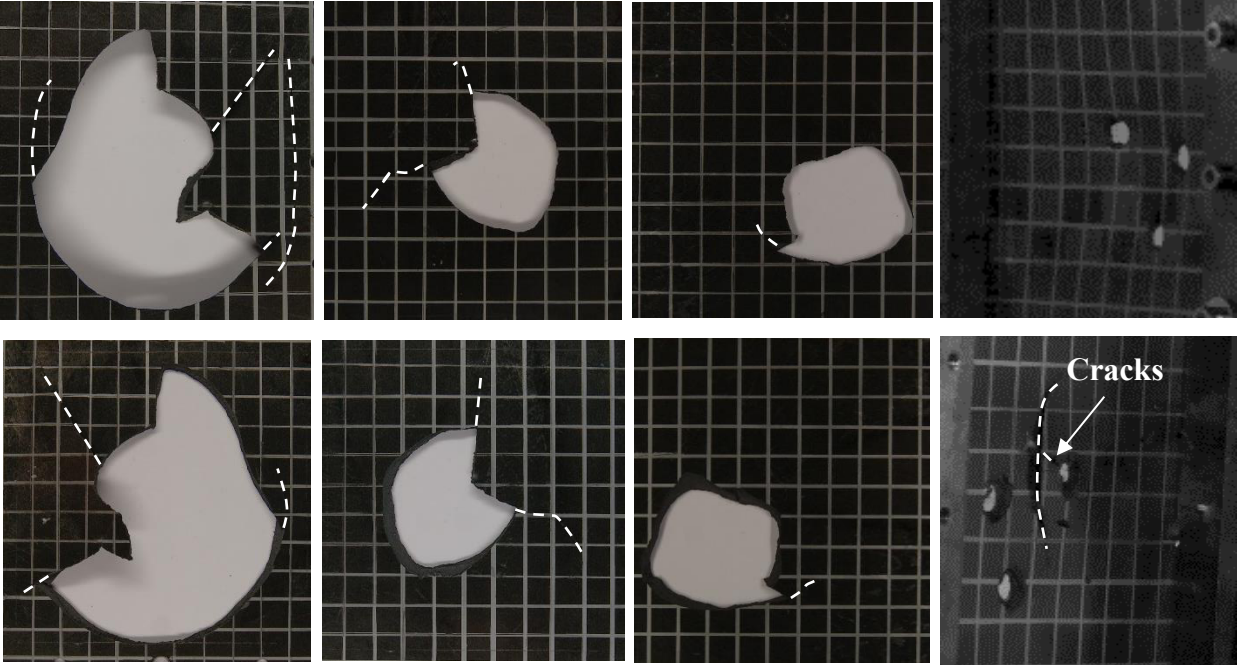
Cracks
Impact velocity increase
(a)
(b)
(c)
(d)

TABLES

Table 1

Table 1
Material properties of SCFR PEEK [16].

	SCFR PEEK composite (CF30)	
	Transversal	Longitudinal
Density (kg/m^3)	1400	
Tensile elastic modulus (GPa)	12.6	24
Compressive elastic modulus (GPa)	15	44
Poisson's rate	0.38	0.385
Yield stress (MPa)	130	180
Tensile strength (MPa)	148	214
Compressive strength (MPa)	174	239
Elongation at break (%)	1.9	2.0

Appendix A. Summary of the experimental data collected from single, sequential and simultaneous impact tests.

Table A1.
Results of single (A) and sequential impacts tests (A+B+C).

Specimen	Test	Impact velocity, V_0 (m/s)	Residual velocity, V_r (m/s)	Kinetic energy (J)	Energy absorption (J)	Damage area (mm^2)
1	A	119.5	0.0	12.2	12.2	988.7
	B	113.0	0.0	10.9	10.9	395.8
	C	90.0	0.0	6.9	6.9	284.8
2	A	168.3	0.0	24.2	24.2	2905.9
	B	167.6	104.0	24.0	14.8	194.2
	C	159.0	55.0	21.6	19.0	1878.5
3	A	195.0	0.0	32.5	32.5	6653.2
	B	-	-	-	-	-
	C	-	-	-	-	-
4	A	271.0	185.0	62.8	33.5	582.6
	B	288.0	203.0	70.9	35.7	113.2
	C	288.8	208	71.3	34.3	80.4
5	A	368.3	313.3	116	32.1	95.0
	B	353.0	295.0	106.5	32.1	91.2
	C	360.5	304.5	111.0	31.8	92.9
6	A	463.6	399.0	183.8	47.6	84.7
	B	469.6	397.0	188.5	53.8	87.5
	C	473.9	402.0	192.0	53.8	88.8

Table A2.
Results of three-projectile simultaneous impacts tests.

Specimen	Sabot velocity, V_0 (m/s)	Residual velocity, V_r (m/s)	Kinetic energy (J)	Energy absorption (J)	Damage surface (mm^2)
1	131.2	15.4	14.7	14.5	6322.9
		17.5	14.7	14.5	
		25.0	14.7	14.2	
2	151.8	7.4	19.7	19.7	1516.0
		84.2	19.7	13.6	
		96.7	19.7	11.7	
3	184.5	75.4	29.1	24.3	1677.2
		88.3	29.1	22.4	
		89.8	29.1	22.2	
4	249.4	174.9	53.2	27.0	269.4
		172.0	53.2	27.0	
		177.2	53.2	26.3	